(4)

Flow Technical Report No. 477

NUMERICAL CALCULATIONS OF THE COLLAPSE OF A CAVITY IN THE VICINITY OF A COMPLIANT WALL

J. H. Duncan

April 1989

Prepared for
OFFICE OF NAVAL RESEARCH
Under Contract No. N00014-85-C-0747

FLOW RESEARCH, INC.
21414 - 68th Avenue South
Kent, Washington 98032
(206) 872-8500

REPORT DOCUMENTATION PAGE

Form Approved OMB No. 0704-0188

1a. REPORT SECURITY CLASSIFICATION: Unclassified	1b. RESTRICTIVE MARKINGS
2a. SECURITY CLASSIFICATION AUTHORITY	3. DISTRIBUTION/AVAILABILITY OF REPORT
2b. DECLASSIFICATION/DOWNGRADING SCHEDULE	
4. PERFORMING ORGANIZATION REPORT NUMBER(S): Flow Technical Report No. 477	5. MONITORING ORGANIZATION REPORT NUMBER(S)
6a. NAME OF PERFORMING ORGANIZATION: Flow Research, Inc. / 6b. OFFICE SYMBOL (If applicable): NA	7a. NAME OF MONITORING ORGANIZATION: DCASMA-Seattle
6c. ADDRESS (City, State, and ZIP Code): 21414 68th Ave. South, Kent, Washington 98032	7b. ADDRESS (City, State, and ZIP Code): Building 5D, Naval Station, Seattle, Washington 98115-5010
8a. NAME OF FUNDING/SPONSORING ORGANIZATION: Office of Naval Research / 8b. OFFICE SYMBOL (If applicable): N00014	9. PROCUREMENT INSTRUMENT IDENTIFICATION NUMBER: N00014-85-C-0747
8c. ADDRESS (City, State, and ZIP Code): Dept. of the Navy Code 1513:GDB, 800 N. Quincy St., Arlington, VA 22217-5000	10. SOURCE OF FUNDING NUMBERS: PROGRAM ELEMENT NO. / PROJECT NO. / TASK NO / WORK UNIT ACCESSION NO.

11. TITLE (Include Security Classification): Numerical Calculations of the Collapse of a Cavity in the Vicinity of a Compliant Wall

12. PERSONAL AUTHOR(S): James H. Duncan

13a. TYPE OF REPORT	13b. TIME COVERED	14. DATE OF REPORT (Year, Month, Day)	15. PAGE COUNT
Final	FROM 8-1-85 TO 11-30-88	4-27-89	22

16. SUPPLEMENTARY NOTATION

17. COSATI CODES			18. SUBJECT TERMS (Continue on reverse if necessary and identify by block number)
FIELD	GROUP	SUB-GROUP	

19. ABSTRACT (Continue on reverse if necessary and identify by block number)

The collapse of a spherical vapor cavity in the vicinity of a compliant boundary is examined numerically. The fluid is treated as a potential flow. Lagrangian boundary conditions are used on the cavity surface; fluid particles and the velocity potential on the surface are tracked in time. At each time step an integral method is used to solve Laplace's equation. The compliant wall is modeled as a membrane with a spring foundation. At the interface between the fluid and the membrane, the pressure and vertical velocity in the flow is matched to the pressure and vertical velocity of the membrane. These boundary conditions are linearized and applied at the position of the undisturbed interface between the flow and the membrane. The results of a preliminary set of calculations are presented in which the initial cavity position and radius, the ratio of the time scale for a spherical collapse to the membrane's spring-mass time scale, and the ratio of the spring constant to the membrane tension are all held constant. The characteristics of the collapse as a function of the ratio of the spring constant to the fluid pressure far from the cavity are examined. It is shown that as the spring constant is reduced, the collapse characteristics change from those of a cavity adjacent to a rigid wall and tend toward those of a cavity in an infinite fluid.

20. DISTRIBUTION/AVAILABILITY OF ABSTRACT	21. ABSTRACT SECURITY CLASSIFICATION	
☒ UNCLASSIFIED/UNLIMITED ☐ SAME AS RPT. ☐ DTIC USERS	Unclassified	
22a. NAME OF RESPONSIBLE INDIVIDUAL: Dr. Choung M. Lee	22b. TELEPHONE (Include Area Code): (202) 696-4305	22c. OFFICE SYMBOL: n00014

DD Form 1473, JUN 86 — Previous editions are obsolete. — SECURITY CLASSIFICATION OF THIS PAGE: Unclassified

TABLE OF CONTENTS

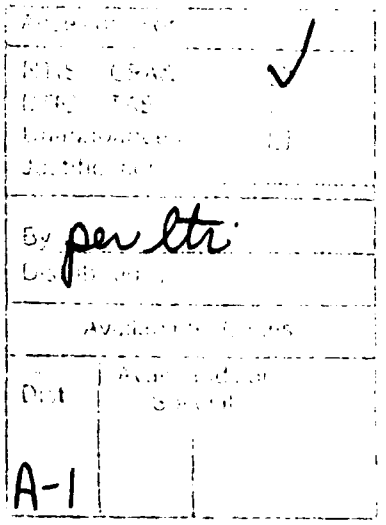

1 Introduction

The collapse of vapor cavities in the vicinity of rigid walls has been the subject of a number of theoretical, numerical and experimental investigations [1,2,3,4,5,6]. The collapse is characterized by a jet which is formed at the side of the cavity farthest from the rigid wall and is directed toward the wall. It is believed that this jet enhances the erosion of solid material from the wall. Several investigators have reported that laboratory cavitation erosion tests of relatively rigid surfaces coated with soft elastomeric materials show increased resistance to erosion [7,8,9]. To explore the mechanism for this phenomenon Gibson and Blake [10] photographed the collapse of a cavity in the vicinity of walls covered by elastomeric coatings of several compositions. They found that under some circumstances the the collapse was modified such that a jet was formed on the side of the cavity closest to the wall and was directed away from the wall. It is theorized that this redirection of the jet protects the wall from erosion. To analyze this effect theoretically they devised a simple model. First, using data from the collapse of a spherical cavity in an infinite fluid, they computed the average pressure force and average displacement on an imaginary surface at the position where the wall would be located in the interactive case. Then using a one-dimensional spring-mass-damper model of the coating, they found coating designs whose impedance matched the average force and average displacement characteristics in the spherical collapse. In this way they attempted to find the coating properties that would make the collapse spherical when the cavity was adjacent to the compliant wall. It was theorized that further changes in the wall properties would direct the jet away from the wall as occurs when the cavity collapses near a free surface. This analysis was a good first attempt and indicated a tentative beneficial parameter range for the coatings.

The computational models for the collapse of a cavity in the vicinity of a rigid wall [1,2,5] or a free surface [11,12] have become quite advanced. In these models the fluid motion is assumed to be inviscid and incompressible and the fluid velocity is obtained from the gradient of a scalar Eulerian velocity potential which satisfies Laplace's equation. Fluid particles on the free surfaces are tracked in time and Bernoulli's equation is used to obtain the velocity potential at the position of these particles. At each time step an integral equation is solved to obtain the value of the fluid velocity in the direction normal to the surfaces. The rigid surface is usually simulated with an image cavity.

In the present paper, in order to compute the collapse of a cavity near a compliant wall, the above model for the fluid motion has been coupled to a simple model of a compliant coating. Specifically, the coating is modeled as a membrane with a spring foundation. This coating is characterized by its mass per unit area (m), membrane tension (T) and spring stiffness per unit area (K). The coating is coupled to the flow model through the normal velocity and the pressure at the flow-coating interface. Linearized boundary conditions are applied at the location of the undisturbed membrane surface. This model is fully interactive. It is shown later in this paper that there are four dimensionless parameters controlling the characteristics to the collapse. These are $R_0/Z_0, T_m/T_0, R_0^2K/T$ and $KR_0/\Delta P$ where R_0 is the initial cavity radius, Z_0 is the initial distance of the center of the cavity from the wall, $T_0 = R_0\sqrt{\rho/(P_\infty - P_0)}$ is the time scale for collapse of the cavity in an infinite fluid, $T_m = \sqrt{m/K}$ is the characteristic spring-mass time scale for the coating, ρ is the density of the fluid, P_∞ is the pressure of the fluid far from the cavity, and P_0 is the pressure in the cavity which is assumed constant. Results of the first computations from the model are presented herein. In these calculations, $R_0/Z_0, T_m/T_0$ and R_0^2K/T were held constant at $1.5, 1.0$ and 12.5 respectively while $KR_0/\Delta P$ was varied from ∞ (a rigid wall) to 12.5. More extensive calculations are underway at the present time.

The remainder of the paper is organized as follows. In Section 2, a description of the mathematical formulation of the full interaction problem is given. This is followed in Section 3 by a description of the numerical implementation of this theory. In Section 4, the results are presented and finally, the conclusions of the work are given in Section 5.

2 Mathematical Formulation

A schematic showing the initial position of the cavity, the compliant wall and the coordinate system used in the calculations is given in Figure 1. A cylindrical coordinate system is used with the z-axis piercing the center of the cavity and directed normal to the undisturbed surface of the compliant wall which is located at $z = 0$. In this coordinate system the problem is axisymmetric about the z-axis. The cavity is initially ($t = 0$) spherical with radius R_0, its maximum value, and its center is located at Z_0. For times before the initial instant the

pressure everywhere in the fluid is P_∞ and the cavity surface is rigid. The internal pressure in the cavity is assumed constant, P_0, for all time. For $t \geq 0$ the boundary of the cavity is a free surface and the pressure in the fluid far from the cavity is constant with value P_∞. The theoretical model for the fluid is similar to the one used by a number of investigators including, most recently, Blake, Taib, and Doherty [11]. The fluid motion is assumed to be incompressible and inviscid and therefore satisfies Laplace's equation:

$$\nabla^2 \phi = 0 \tag{1}$$

where ∇ is the gradient operator, ϕ is the the velocity potential and $\vec{u} = \nabla\phi$ where $\vec{u}$ is the fluid velocity. On the surface of the cavity the pressure in the fluid must equal the pressure in the cavity, P_0. This can be written as Bernoulli's equation in material derivative form:

$$\frac{D\phi}{Dt} = \frac{1}{2}|\nabla\phi|^2 + \frac{P_\infty - P_0}{\rho} \tag{2}$$

where D/Dt is the derivative with respect to time following a fluid particle. The kinematic boundary condition on the surface of the cavity states that material points remain on the surface of the cavity:

$$\frac{D\vec{x_c}}{Dt} = \nabla\phi \tag{3}$$

where $\vec{x_c}$ is the position vector to these material points.

The wall is modeled as a membrane with tension T and mass per unit area m that is supported by a spring foundation of spring constant K. The equation describing the motion of the membrane is

$$m\frac{\partial^2\eta}{\partial t^2} - T\frac{1}{r}\frac{\partial}{\partial r}(r\frac{\partial\eta}{\partial r}) + K\eta = -P_c(r,t) \tag{4}$$

where $\eta = \eta(r,t)$ is the vertical displacement of the membrane surface and P_c is the pressure on the membrane. The fluid and the membrane are coupled using linearized equations for the pressure and velocity in the two systems. These equations are satisfied at the undisturbed position of the coating surface $z = 0$:

$$\frac{\partial\eta}{\partial t} = u_z(r,0,t) \tag{5}$$

$$P_c(r,t) = P(r,0,t) \tag{6}$$

For $t < 0$ the the springs are compressed uniformly due to the uniform pressure P_∞ applied by the fluid. The position of the membrane at this time is taken as $z = 0$.

The time marching procedure to solve this problem is as follows. Assume that at time t all dependent variables are known. The boundary conditions on the surface of the cavity, Equations (2) and (3), are integrated numerically to get the position of the surface of the cavity and the value of ϕ on the cavity at time $t + \Delta t$. The membrane equation can be used to obtain the value of $\partial\eta/\partial t = \partial\phi/\partial n$ at the membrane surface at $t + \Delta t$. In order to move on to the next time step, $t + 2\Delta t$, the values of $\nabla\phi$ must be known on the cavity surface for use in Equations (2) and (3). However, at this point only the value of $\partial\phi/\partial s$ is known (where s is a coordinate along the cavity surface). Also, in order to find the value of $\partial\phi/\partial n$ on the membrane surface at $t+2\Delta t$, the pressure must be known on the membrane surface at $t+\Delta t$ for use in Equation (4). The pressure at $t + \Delta t$ can be obtained from Bernoulli's equation if $\partial\phi/\partial t$ and $\nabla\phi$ are known. Since $\partial\phi/\partial n$ on the membrane surface has been computed from integrating the membrane equation in time and ϕ at time t is known, only the value of ϕ on the membrane at time $t + \Delta t$ remains to be computed, then $\partial\phi/\partial s$ and $\partial\phi/\partial t$ can be computed from finite difference. Thus, to complete the problem, the values of $\partial\phi/\partial n$ on the cavity surface and ϕ on the membrane surface are obtained by solving Laplace's equation in the form of the integral equation:

$$\int_{S_c+S_m} \frac{\partial g(\vec{p},\vec{q})}{\partial n}\phi(\vec{q})dS_q - \int_{S_c+S_m} g(\vec{p},\vec{q})\frac{\partial\phi}{\partial n}dS_q = 2\pi\phi(\vec{p}) \tag{7}$$

where S_c is the surface of the cavity, S_m the interface between the coating and the fluid, $\vec{p}$ is a field point that is on the surface $S = S_c + S_m$, $\vec{q}$ is the source point that is also on S, $g(\vec{p},\vec{q}) = 1/|\vec{p} - \vec{q}|$ and dS_q is the area element of S varying the point $\vec{q}$. Once this equation is solved the calculation can proceed on to the next time step or, with a companion form of this integral equation, the velocity and pressure can be found at any point in the fluid.

3 Numerical Implementation

In the numerical model the surface of the cavity is approximated by a set of surfaces (panels) each of which is obtained by rotating a straight line in the $r - z$ plane about the z-axis (see Figure 2). The cavity is composed of n_b of these panels. The bottom boundary of the fluid is modeled by a is set of n_w of these panels located at $z = 0$ with normal in the z-direction. Assume that at any time, t_i, (the subscript is used to denote the time step) the dependent variables describing the flow and the membrane wall are completely know and it is desired to advance to the next time step, t_{i+1}. The r, z coordinates at t_{i+1} of the $n_b + 1$ intersections

(nodes) of the lines joining adjacent panels on the cavity with the $r-z$ plane are found from the finite difference form of Equations (3):

$$r_{i+1}^j = r_i^j + u_i^j(t_{i+1} - t_i) \tag{8}$$

$$z_{i+1}^j = z_i^j + w_i^j(t_{i+1} - t_i) \tag{9}$$

where the superscript j refers to the node (see Figure 2). The value of ϕ at t_{i+1} at each node is obtained from the finite difference form of Equation (2)

$$\phi_{i+1}^j = \phi_i^j + \left(\frac{1}{2}|\nabla\phi_i^j|^2 + \frac{P_\infty - P_0}{\rho}\right)(t_{i+1} - t_i) \tag{10}$$

At this point we have the position of the nodes on the cavity and the value of ϕ at each node at t_{i+1}. The next step is to obtain $\partial\phi\ \partial n$ at the nodes on the membrane-flow interface.

The first step in the solution of the membrane problem is to Hankel transform Equation (4). After combining Equation (6) with the membrane equation (4) and performing the Hankel transform, the membrane equation becomes

$$m\frac{\partial^2\bar{\eta}}{\partial t^2} + T\bar{\eta} + K\bar{\eta} = -\bar{P}(k,0,t) \tag{11}$$

where for any quantity Q the Hankel transform is given by:

$$\bar{Q}(k,z,t) = \int_0^\infty Q(r,z,t)\, rJ_0(kr)dr \tag{12}$$

and k is called the wavenumber. The values of $\bar{\eta}_{i+1}$ at each wavenumber k^j are obtained from the temporal finite difference form of Equation (11) :

$$\bar{\eta}_{i+1}^j = (2 + (T(k^j)^2 + K)\frac{\Delta t^2}{m})\bar{\eta}_i^j - \bar{\eta}_{i-1}^j - \frac{P_i^j}{m}\Delta t^2 \tag{13}$$

The values of η_{i+1}^j at the nodes between wall panels are then obtained by inverting the Hankel transform. The Hankel transforms are performed using a numerical algorithm described by Anderson [13]. The vertical velocity at the coating surface is then

$$\frac{\partial\eta}{\partial t} \simeq \frac{\partial\phi}{\partial n} \simeq \frac{\eta_{i+1}^j - \eta_i^j}{\Delta t} \tag{14}$$

Thus after this computation the position and the values of ϕ are known for the nodes on the cavity and the values of $\partial\phi/\partial n$ are known for the nodes on the membrane. In order to

advance to the next time step the values of $\partial\phi/\partial n$ on the cavity surface and the values of ϕ on the membrane surface must be computed from Equation (7). In the numerical solution of this integral equation the values of ϕ and $\partial\phi/\partial n$ are assumed to vary linearly in the r, z plane along each panel. Thus, in its discrete form the integral equation becomes

$$\alpha^i\phi^i = \sum_{j=1}^{j=N}\left(G^{1,i,j}\left(\frac{\partial\phi}{\partial n}\right)^j + G^{2,i,j}\left(\frac{\partial\phi}{\partial n}\right)^{j+1}\right) - \sum_{j=1}^{j=N}\left(GN^{1,i,j}\phi^j + GN^{1,i,j}\phi^{j+1}\right) \tag{15}$$

where $N = n_c + n_m$ and

$$G^{1,i,j} = \int_0^{L^j} dl^j \frac{L^j - l^j}{L^j}\int_0^{2\pi}\frac{1}{|\vec{p^i} - \vec{q^j}(r,\theta)|}d\theta \tag{16}$$

$$G^{2,i,j} = \int_0^{L^j} dl^j \frac{l^j}{L^j}\int_0^{2\pi}\frac{1}{|\vec{p^i} - \vec{q^j}(r,\theta)|}d\theta \tag{17}$$

$$GN^{1,i,j} = \int_0^{L^j} dl^j \frac{L^j - l^j}{L^j}\int_0^{2\pi}\frac{\partial}{\partial n}\frac{1}{|\vec{p^i} - \vec{q^j}(r,\theta)|}d\theta \tag{18}$$

$$GN^{2,i,j} = \int_0^{L^j} dl^j \frac{l^j}{L^j}\int_0^{2\pi}\frac{\partial}{\partial n}\frac{1}{|\vec{p^i} - \vec{q^j}(r,\theta)|}d\theta \tag{19}$$

In these equations the length of panel j in the $r - z$ plane is given by L^j and dl^j is the corresponding differential length element. The parameter α^i is a geometrical parameter. On the flow-membrane interface, which is taken at $z = 0$, a tangent plane to the paneled surface exists at each node and $\alpha_i = 2\pi$ for these nodes ($n_c + 2 \leq j \leq n_c + n_m + 2$) as it would on a continuous surface. However, for the nodes on the cavity surface, there is no tangent plane and $\alpha^i = \lim_{\epsilon\to\infty} A_f/\epsilon^2$ where ϵ is the radius of a small sphere centered on the node i and A_f is the portion of the surface area of the sphere that is in the fluid.

Starting the calculations at $t = 0$ has turned out to be rather difficult. The problem lies in the value of the pressure on the membrane at $t = 0$. Since the values of ϕ on the cavity and $\partial\phi/\partial n$ on the membrane are zero at $t = 0$, use of the integral equation will yield $\phi = 0$ on the membrane at this time. Thus, from Bernoulli's equation, the pressure on the membrane at $t = 0$ is determined by $\partial\phi/\partial t$. To compute this derivative the values of ϕ at $t = \Delta t$ must be determined. In proceeding to time Δt to obtain the required values of ϕ on the membrane, the position of the nodes on the cavity and the corresponding values of ϕ are obtained from Equations and (8) and (10). In order to get ϕ on the membrane surface the value of $\partial\phi\partial n$ must be known there so that the integral equation (15) can be

solved. However, $\partial\phi\partial n$ is computed from the membrane velocity and this value requires the pressure on the membrane at $t = 0$. Unfortunately, this pressure is the quantity that we have been trying to compute in the first place. An iterative scheme was devised to overcome this problem. On the first iteration, the pressure on $z = 0$ at $t = 0$ is computed assuming the coating to be rigid. This allows for the computation of $\partial\phi\partial n$ on the membrane at $t = \Delta t$. It has been found that the distribution of the pressure on the membrane oscillates from one time step to the next with this starting pressure assumption. However, if the membrane wall is stiff enough, the pressure seems to settle down to a constant distribution after several time steps. For these stiff coatings, the calculation was restarted at this point with the equilibrated pressure distribution rather than the rigid wall distribution used at $t = 0$. For walls that are more compliant, the pressure distribution diverges when starting with the rigid wall pressure distribution. Thus, in order to perform the calculation in these cases, the calculation was started with a stiff wall and after several time steps, when the pressure equilibrated, the calculation was restarted with less stiff wall parameters. This procedure was repeated until the desired wall properties were reached.

4 Results

There are a number of independent variables in the the cavity collapse problem. For the fluid, these variables include the initial cavity radius, R_0, and distance from the wall, Z_0, the pressure difference, $P_\infty - P_0$ and the density of the fluid, ρ. For the membrane the variables are the mass per unit area, m, the tension, T, and the spring constant, K. Thus, the collapse time, T_c, is a function of seven independent parameters which contain the dimensions of mass, length and time. In dimensionless form there are five independent parameters and if we define $T_0 = R_0\sqrt{\rho/(P_\infty - P_0)}$, (the characteristic time scale for the collapse of a cavity in an infinite fluid) and $T_m = \sqrt{m/K}$, (the characteristic spring-mass time scale for the coating), we find:

$$\frac{T_c}{T_0} = f\left(\frac{R_0}{Z_0}, \frac{T_m}{T_0}, \frac{R_0^2 K}{T}, \frac{K R_0}{\Delta P}\right) \tag{20}$$

where $\Delta P = P_\infty - P_0$. In the following we have varied only $KR_0/\Delta P$ with the other dimensionless parameters held constant: $R_0/Z_0 = 2/3$, $T_m/T_0 = 1$, and $R_0^2 K/T = 12.5$. In these calculations, the cavity is composed of 32 panels which are of equal arc in the $r - z$ plane when the cavity is spherical. There are 70 panels on the flow-membrane interface. These

panels do not move from there positions at $t = 0$. The first node on this interface is at $r = 0$, and the next is at $r = 0.05R_0$. The length of subsequent panels increases linearly with the last node at $r = 100.0R_0$. In these initial calculations the time step was constant throughout the collapse and equal to $0.00125T_0$. Because the rate of change of ϕ increases rapidly toward the end of the collapse while the time step is constant, the calculations become inaccurate just before the collapse is complete. It is estimated that inaccuracies become important at about a time of $0.02T_0$ before the end of the collapse. At the present time a variable time step version of the computer program is under development to remedy this problem. However, the results in the following discussion, which show for instance the collapse time of the cavity as a function of coating properties, are still valid for comparison purposes.

Figure 3 contains profiles of the cavity at various times during the collapse for the case of a rigid wall, $KR_0/\Delta P = \infty$, and the case of a compliant wall $KR_0/\Delta P = 12.5$. Note that the profiles appear fairly similar except that the collapse occurs over a longer time for the case with the rigid wall. Note also that the vertical extent of the cavity at the final instant is greater for the case with the rigid wall and that the height, z_c, where the upper (north) pole of the cavity meets the lower (south) pole of cavity is larger for the compliant wall case. To emphasize this later point plots of the the height of the north and south poles of the cavities versus time for the rigid wall case and cases with $KR_0/\Delta P = 50.0, 25.0$, and 12.5 are shown in Figure 4. Note the trend toward larger values of z_c and shorter collapse times as $KR_0/\Delta P$ is decreased from ∞ (the a rigid wall) to 12.5. For the rigid wall, $z_c = 1.035R_0$ and $T_c = 1.035T_0$, while for the case with $KR_0/\Delta P = 12.5$, $z_c = 1.128R_0$ and $T_c = 0.936T_0$. In the case of a cavity collapsing in an infinite fluid the collapse time is $0.915T_0$ and z_c would equal $Z_0 = 1.5$. Thus, the trend is toward the infinite fluid case as $KR_0/\Delta P$ is decreased.

The pressure distributions $(P(r) - P_\infty)/(P_\infty - P_0)$ on the flow-membrane interface at times corresponding to Figure 3 are shown in Figure 5 for the case with the rigid wall and the case with $KR_0/\Delta P = 12.5$. Note that the plots only extend to $r = 20R_0$ while the wall panels extend to $r = 100R_0$. In both cases the pressure is initially slightly negative directly under the cavity and becomes positive with a value of about 15.0 toward the end of the collapse. At first glance the shapes of these distributions seem fairly similar. However, the values at $r/R_0 = 20.0$ are negative on the compliant wall and positive on the rigid wall. Since the horizontal derivative of the pressure is about the same, the component of the flow

tangent to the wall is outward and must be of about the same magnitude in the two cases. In the compliant wall case the gradient must eventually change sign in order to reach zero at $r = \infty$ indicating flow toward the $z-$axis. In Figure 6 the pressure on the membrane at $r = 0$ is plotted versus time for the case with the rigid wall, the cases with $KR_0/\Delta P = 50.0, 25.0,$ and 12.5, and a case with collapse in an infinite fluid (spherical collapse). In the latter case the pressure was evaluated at a distance Z_0 from the center of the spherical cavity. Note that all the curves have about the same shape, but as the wall is softened from a rigid wall to $KR_0/\Delta P = 12.5$ and finally to the spherical case (no wall), the curve is shifted up slightly and to the left. This is a further indication that softening the wall is making the characteristics of the collapse tend toward the spherical collapse case.

The distribution of vertical velocity of the membrane surface at various times is plotted in Figure 7 for two cases. In Figure 7a the full membrane coating interaction was computed for $KR_0/\Delta P = 12.5$. However, in Figure 7b the pressure from the rigid wall calculation was used to drive the membrane, also with $KR_0/\Delta P = 12.5$. (The membrane motion was not fed back to the flow model in this partial interaction case.) Again the curves for the two cases look similar. However, the velocities for the partial interaction case are larger at $r = 20R_0$. The maximum value of the membrane displacements corresponding to this data is about $0.025R_0$. Since the horizontal length scale of the membrane deformations is R_0, the deformations are of exceedingly small slope and the linearization of the boundary conditions at the flow coating interface is justified. Plots of the velocity at $r = 0$ versus time for the full interaction cases with $KR_0/\Delta P = 50.0, 25.0,$ and 12.5, the partial interaction case, and the fluid velocity at a distance Z_0 from a spherical collapse are shown in Figure 8. Note that, as expected, the velocity increases with time and increases as the spring stiffness, $KR_0/\Delta P$, decreases. The partial interaction case and the corresponding full interaction case are identical until about $t/T_0 = 0.6$. However, they are quite different at the end of the collapse. The maximum value of the velocity for the spherical collapse is roughly five times larger than the value for the full interaction with $KR_0/\Delta P = 12.5$. Thus, under the assumption that the collapse will become spherical when the compliant wall behaves in a manner similar to the fluid at that position in a spherical collapse, the wall will have to be considerably softer to prevent the formation of the jet directed toward the wall.

5 Conclusion

A numerical method for the computation of the collapse of a cavity adjacent to a compliant surface has been presented. The results of preliminary calculations show that as the spring-backed membrane becomes soft, the collapse characteristics change in the direction of the collapse of a spherical cavity in an infinite fluid. At the present time calculations for a wider range of conditions are being pursued and the calculation method is being modified to include variable time steps and computations of the energy exchange between the flow and the coating.

Acknowledgements

This work was begun while the author worked at Flow Research Company and was supported by the Office of Naval Research under contract N00014-85-C-0747. The author wishes to acknowledge Georges Chahine for a number of helpful discussions and for suggesting the problem and Ugo Piomelli for several discussions concerning the numerical aspects of the problem.

References

[1] M.S. Plesset and R.B. Chapman, "Collapse of Initially spherical Vapour Cavity in the Neighbourhood of Solid Boundary" *J. Fluid Mech.* Vol. 47, part 2, pp. 283-290 (1970)

[2] L. Guerri and G. Lucca and A. Prosperetti, "A Numerical Method for the Dynamics of Non-spherical Cavitation Bubbles" *Proceedings of the Second International Colloquium on Drops and Bubbles*, Monterey, Calif., 1981.

[3] G. Chahine and A. G. Bovis, "Pressure Field Generated by Nonspherical Bubble Collapse" *Fluids Engineering Division*, 1982

[4] Andrea Prosperetti, "Bubble Dynamics: A Review and Some Results" *Applied Scientific Research* 38:145-164 (1982)

[5] J.R. Blake, B.B. Taib and G. Doherty, "Transient Cavities Near Boundaries. Pat 1. Rigid Boundary", *J. Fluid Mech.*, Vol 170, pp. 479-497 (1986)

[6] Y. Tomita and A. Shima, "Mechanisms of Impulsive Pressure Generation and Damage Pit Formation by Bubble Collapse", *J. Fluid Mech.*, Vol. 169, pp. 535-564 , 1986.

[7] J. Z. Lichtman, "Cavitation Erosion Performance and Related Properties of Cured Sheet Elastomeric Coating Systems" *Journal of Materials*, Vol. 2, No. 3, pp. 638-660, 1967.

[8] W. J. Rheingans, "accelerated Cavitation Research" *Trans. ASME*, Vol. 72, No. 5, pp. 705-719, 1950.

[9] F. J. Dashnaw, A. A. Hochrein, Jr., R. S. Weinreich, P. K. Conn, and I. C. Snell, "Development of Protective Covering Systems for Steel and Bronze Ship Propellers" *Soc. Nav. Arch. Mar. Eng. Annual Meeting*, N.Y., November, 1980.

[10] "The Growth and Collapse of Bubbles Near Deformable Surfaces" *Applied Scientific Research*, Vol. 28, pp. 215-224,1982.

[11] J.R. Blake and D.C. Gibson, "Growth and Collapse of a Vapour Cavity near a free Surface" *J.Fluid Mech.* Vol. 111 pp. 123-140 (1981)

[12] D. G. Dommermuth and D.K.P. Yue "Numerical Simulations of Nonlinear Axisymmetric Flows with a Free Surface" *J. Fluids Mech.* Vol. 178, pp. 195-210, (1987)

[13] W.L. Anderson, "Fast Hankel Transforms Using Related and Lagged Convolutions", *ACM Transactions on Mathematical Software*, Vol. 8 No. 4 pgs. 344-368 (1982)

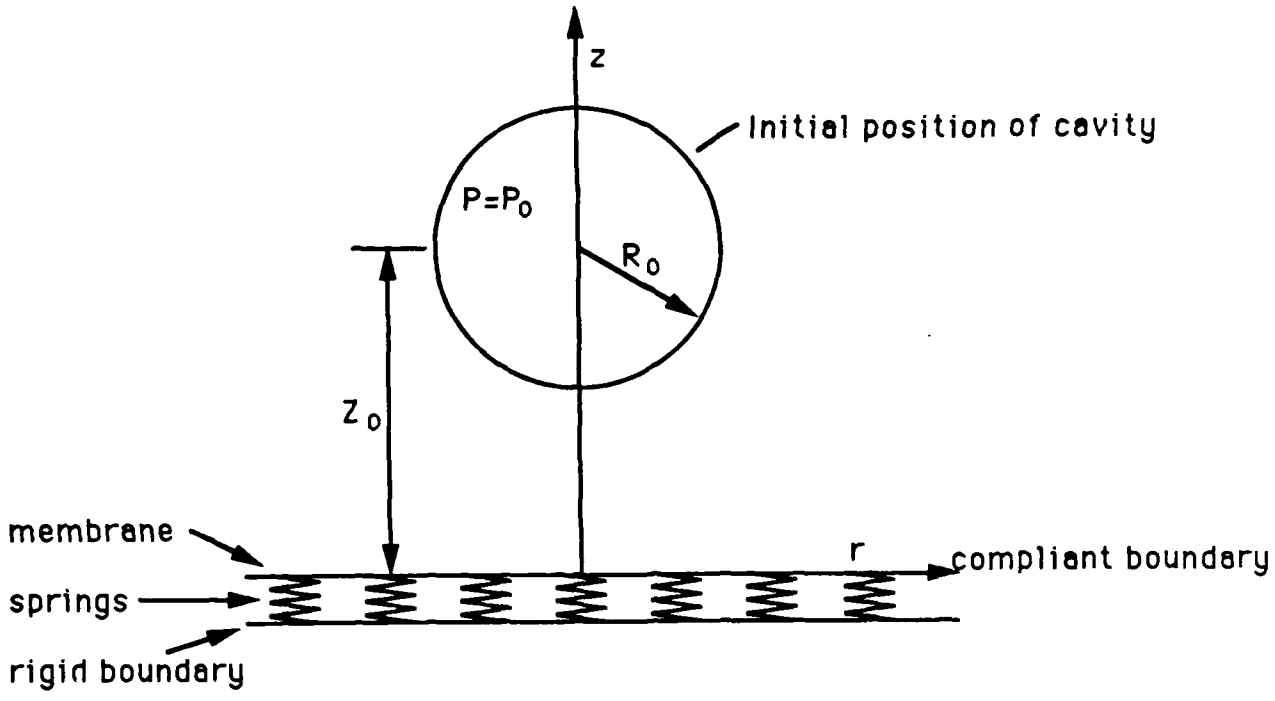

Figure 1 Schematic showing the coordinate system and the initial position of the cavity and the compliant boundary

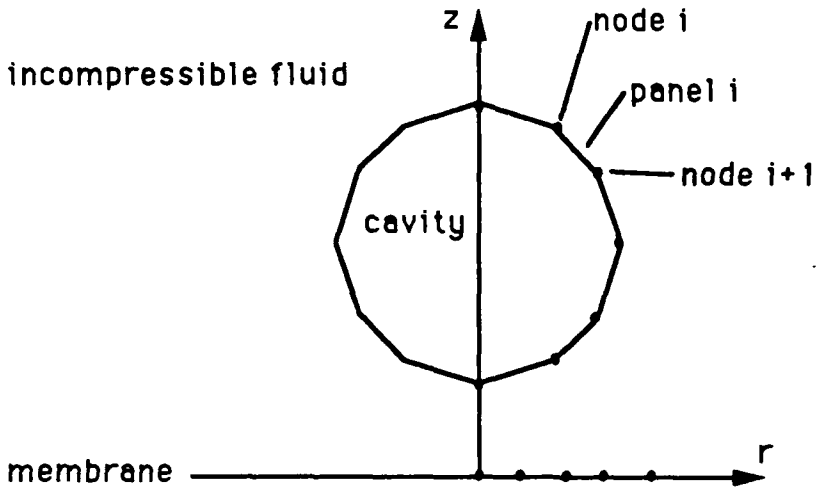

Figure 2 Nodes and panels on the surface of the cavity and the flow membrane interface.

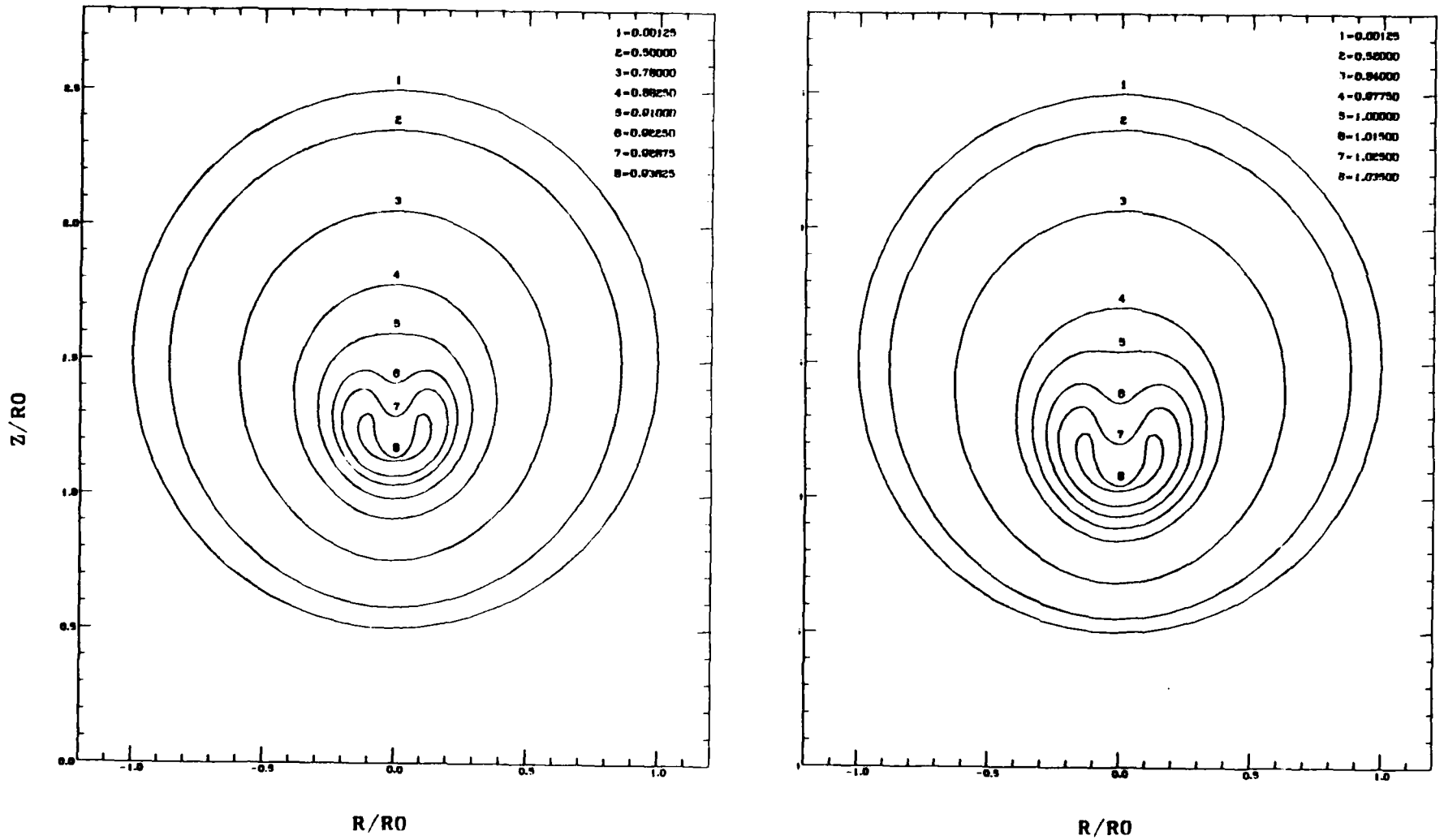

Figure 3. Cavity profiles at various times. a: $R_0/Z_0 = 1.5$, $T_m/T_0 = 1.0$, $R_0^2 K/T = 12.5$, $KR_0/\Delta P = 12.5$. b: rigid wall, $R_0/Z_0 = 1.5$.

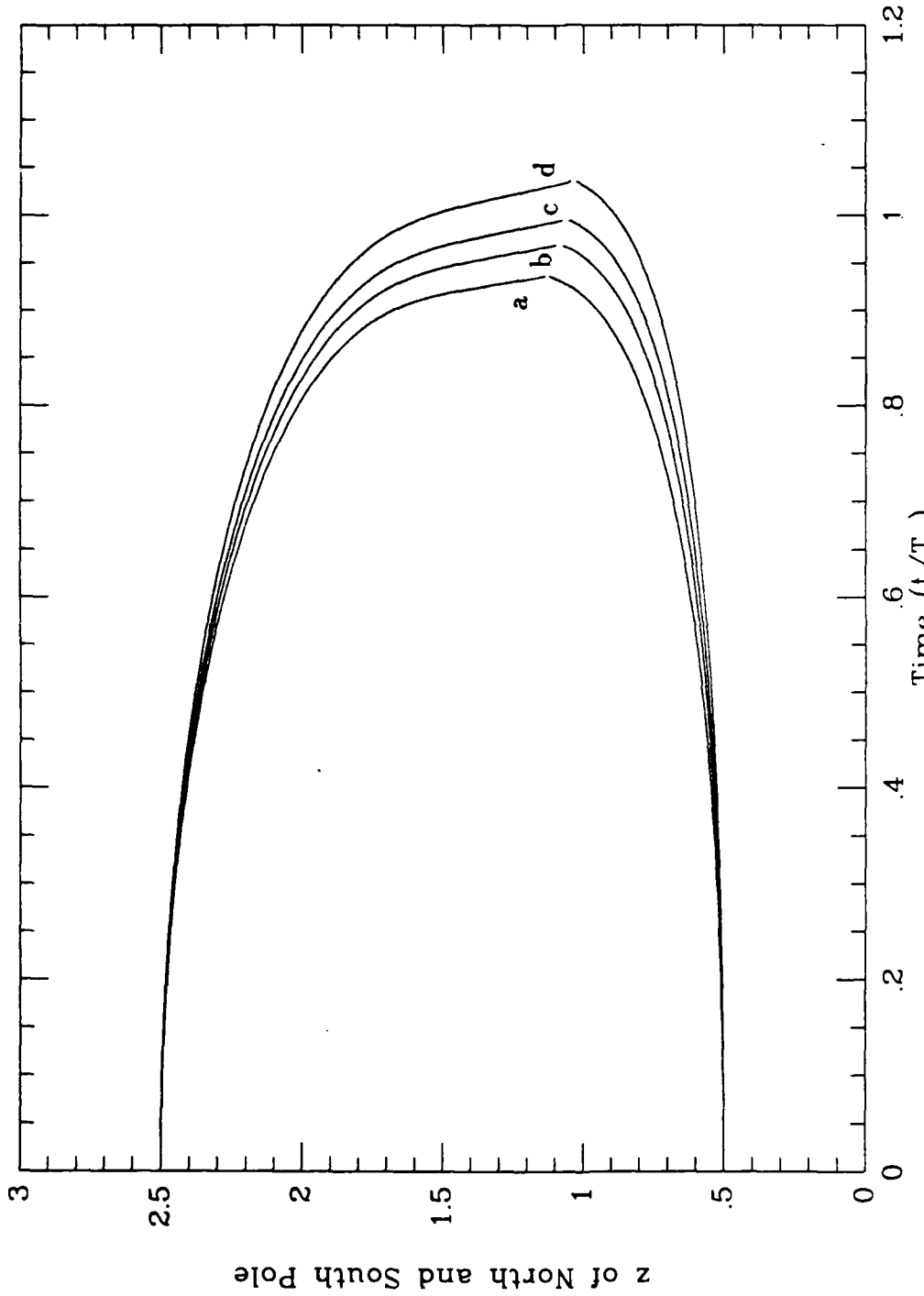

Figure 4. Height of North and South poles of the cavity versus time for four cases. a: $R_0/Z_0 = 1.5$, $T_m/T_0 = 1.0$, $KR_0/\Delta P = 12.5$. b: $R_0/Z_0 = 1.5$, $T_m/T_0 = 1.0$, $R_0^2K/T = 12.5$, $KR_0/\Delta P = 25.0$. c: $R_0/Z_0 = 1.5$, $T_m/T_0 = 1.0$, $R_0^2K/T = 12.5$, $KR_0/\Delta P = 50.0$. d: rigid wall, $R_0/Z_0 = 1.5$.

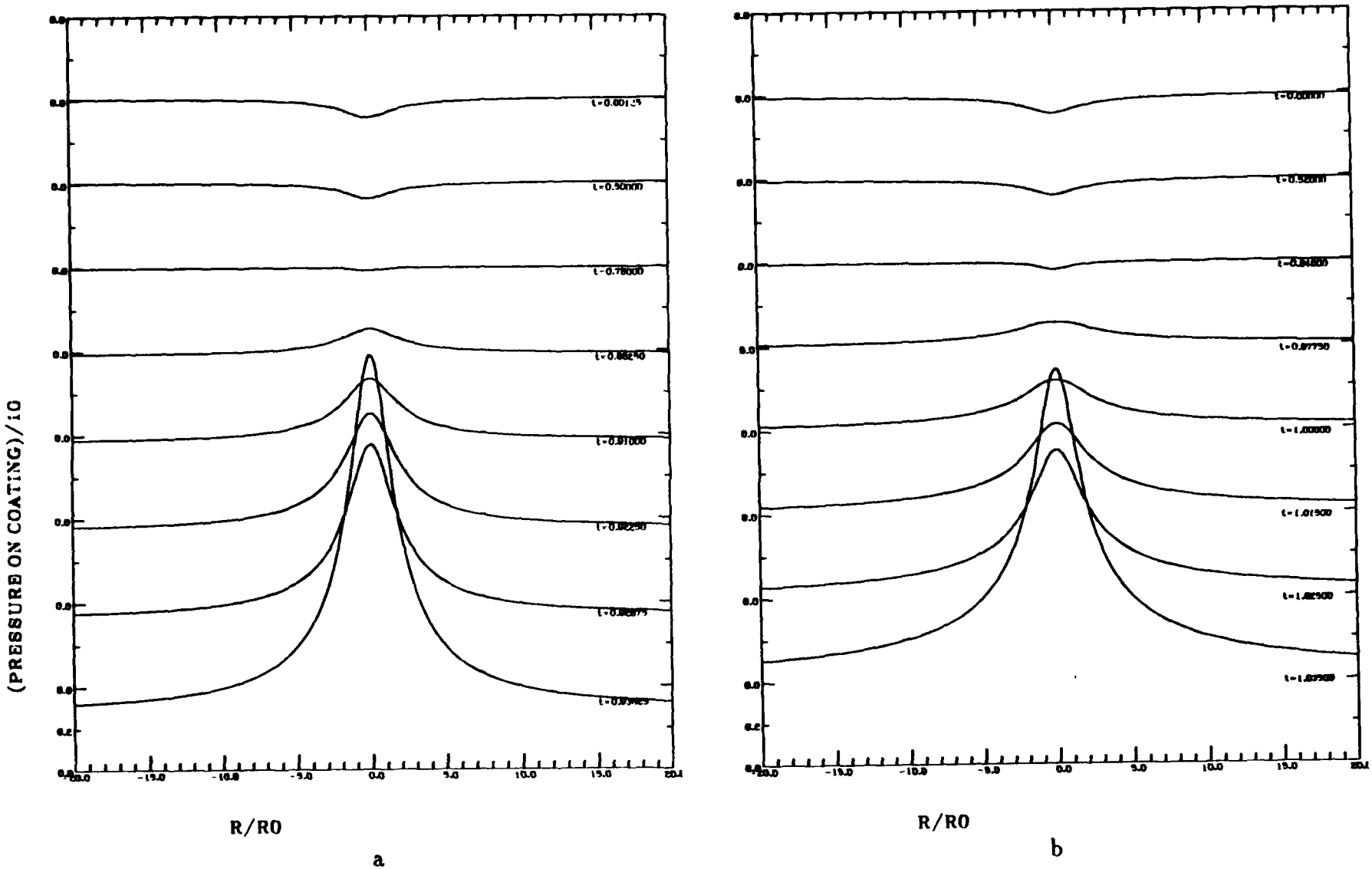

Figure 5. Pressure versus r at $z = 0$ and various times. a: $R_0/Z_0 = 1.5$, $T_m/T_0 = 1.0$, $R_0^2 K/T = 12.5$, $KR_0/\Delta P = 12.5$. b: rigid wall, $R_0/Z_0 = 1.5$.

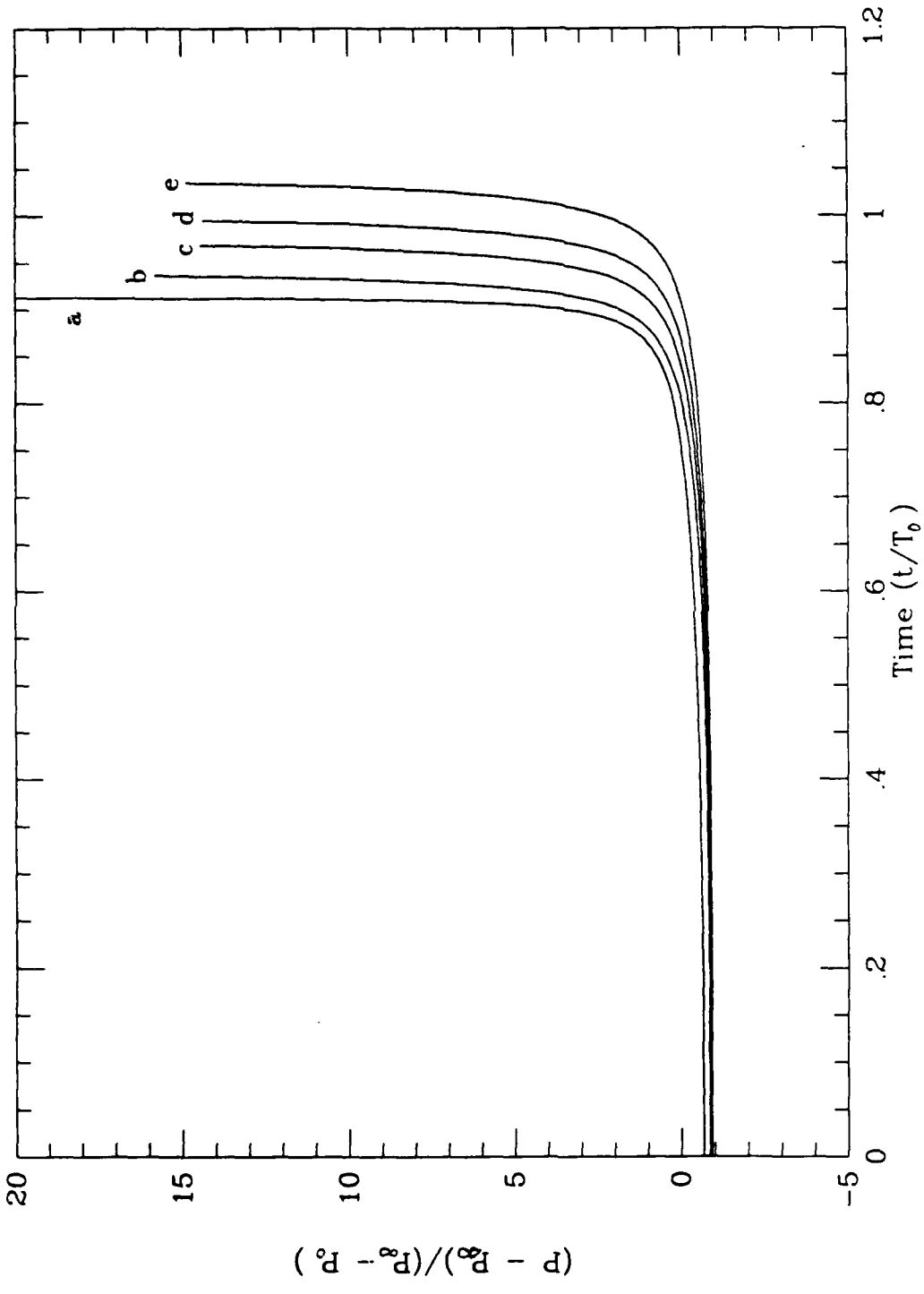

Figure 6. Pressure at $r = 0$ on the membrane surface versus time. a: the pressure at the radius Z_0 for a spherical cavity collapsing in an infinite fluid, b: $R_0/Z_0 = 1.5$, $T_m/T_0 = 1.0$, $R_0^2K/T = 12.5$, $KR_0/\Delta P = 12.5$. c: $R_0/Z_0 = 1.5$, $T_m/T_0 = 1.0$, $R_0^2K/T = 12.5$, $KR_0/\Delta P = 25.0$. d: $R_0/Z_0 = 1.5$, $T_m/T_0 = 1.0$, $R_0^2K/T = 12.5$, $KR_0/\Delta P = 50.0$. e: rigid wall, $R_0/Z_0 = 1.5$.

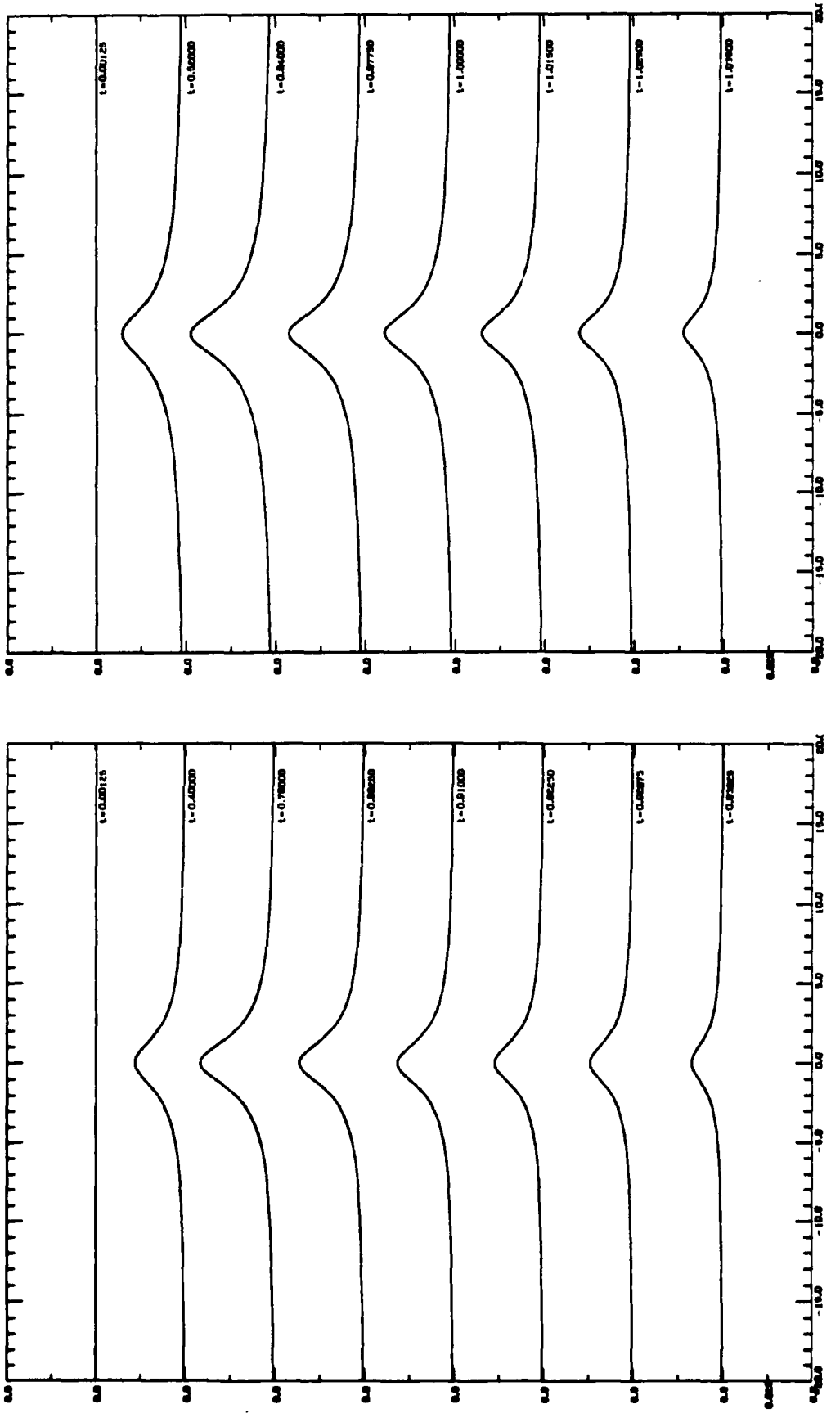

Figure 7. Vertical velocity of the membrane versus radius at various times. a: $R_0/Z_0 = 1.5$, $T_m/T_0 = 1.0$, $R_0^2K/T = 12.5$, $KR_0/\Delta P = 12.5$. b: rigid wall pressure distribution on compliant wall, $R_0/Z_0 = 1.5$, $T_m/T_0 = 1.0$, $R_0^2K/T = 12.5$, $KR_0/\Delta P = 12.5$.

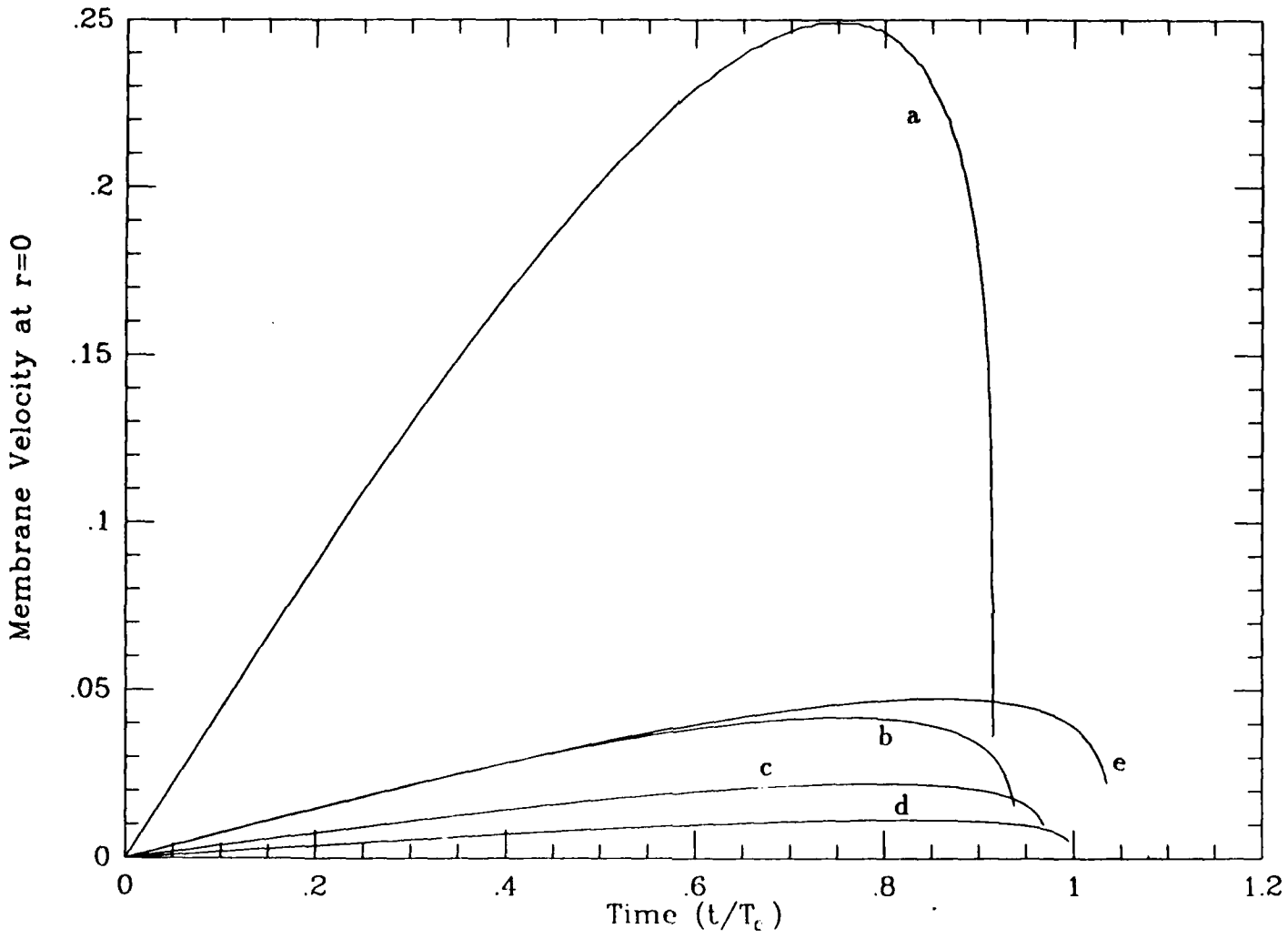

Figure 8. Vertical velocity at $r = 0$ on the membrane surface versus time. a: the velocity at the radius Z_0 for a spherical cavity collapsing in an infinite fluid, b: $R_0/Z_0 = 1.5$, $T_m/T_0 = 1.0$, $R_0^2K/T = 12.5$, $KR_0/\Delta P = 12.5$. c: $R_0/Z_0 = 1.5$, $T_m/T_0 = 1.0$, $R_0^2K/T = 12.5$, $KR_0/\Delta P = 25.0$. d: $R_0/Z_0 = 1.5$, $T_m/T_0 = 1.0$, $R_0^2K/T = 12.5$, $KR_0/\Delta P = 50.0$. e: rigid wall, $R_0/Z_0 = 1.5$.